H1prelim-08-031 Submitted to

XVI International Workshop on Deep-Inelastic Scattering, DIS2008, April 7-11, 2008, London
Parallel Session **Hadronic Final States and QCD**

Electronic Access:https://www-h1.desy.de/publications/H1preliminary.short_list.html

Jet Production at high Q^2 and determination of α_s using the full HERA data

H1 Collaboration

Abstract

High E_T jet production is studied in neutral current deep-inelastic $e^{\pm}p$ scattering at large four momentum transfer squared $Q^2 > 150$ GeV^2 with the H1 detector, using a combined data sample of HERA I and HERA II, corresponding to an integrated luminosity of 395 pb^{-1}. The inclusive jet, 2-jet and 3-jet cross sections, normalized to the neutral current deep-inelastic scattering cross section, referred to as jet multiplicity, 2-jet and 3-jet rates, are measured as a function of Q^2 and of the jet transverse energy in the Breit frame $E_{T,B}$. The measurements are found to be well described by calculations at next-to-leading order in perturbative QCD. The preliminary results on inclusive jets presented here are compared to recently published results, based on HERA I data with an integrated luminosity 65.4 pb^{-1}. The strong coupling α_s is extracted from each of the individual jet measurements as well as from their combination.

1 Introduction

Jet production in neutral current (NC) deep-inelastic scattering (DIS) at HERA provides an important testing ground for Quantum Chromodynamics (QCD). The Born contribution in DIS gives only indirect information on the strong coupling α_s via scaling violations of the proton structure functions and generates no transverse momenta in the Breit frame[1]. Partons with transverse momenta are produced in lowest order (LO) in α_s by the QCD-Compton and boson-gluon fusion processes. Jet production in the Breit frame, therefore, provides direct sensitivity to α_s and allows for a precision test of QCD. Analyses of inclusive jet production in DIS at high four momentum transfer squared Q^2 were previously performed by the H1 and ZEUS collaborations at HERA. The most recently published analyses [3, 4] are based on HERA I 1999-2000 data. Perturbative QCD (pQCD) calculations supplemented with hadronisation corrections were found to describe the data.

2 Event kinematics and selection

The data sample for this analysis was collected with the H1 detector at HERA in the years 1999 to 2000 (HERA I) and 2003 to 2007 (HERA II). During this period, HERA collided positrons or electrons[2] of energy $E_e = 27.6$ GeV with protons of energy $E_p = 920$ GeV giving a centre-of-mass energy $\sqrt{s} = 319$ GeV. The data sample used corresponds to an integrated luminosity of 395 pb^{-1}, shared equally between periods of beams of positrons and electrons.

The DIS phase space covered by this analysis is defined by

$$150 < Q^2 < 15000\,\mathrm{GeV}^2 \qquad 0.2 < y < 0.7 \quad ,$$

where y quantifies the inelasticity of the interaction. These two variables are reconstructed from the four momenta of the scattered positron and the hadronic final state particles using the electron-sigma method [1].

The energy of the scattered electron E'_e is required to exceed 11 GeV and is measured in regions of the calorimeter, where the trigger efficiency is above 98%. The z-coordinate[3] of the event vertex is required to be within ± 35 cm of the average position of the interaction point. This condition reduces contributions of beam induced background and cosmic muons. The total longitudinal energy balance Σ must satisfy $35 < \Sigma = \sum_i (E_i - p_{z,i}) < 65$ GeV, where the sum runs over all detected particles. This requirement reduces the contributions from photoproduction and DIS events with strong initial state radiation. Elastic QED Compton and lepton pair production processes are suppressed by rejecting events containing additional isolated electromagnetic deposits and low hadronic activity. The remaining photoproduction background is estimated using Monte Carlo simulations and is found to be negligible in all Q^2 and $E_{T,B}$ bins.

[1] The Breit frame is a frame where the virtual boson and the proton collide head on.

[2] Unless otherwise stated the colliding lepton is called ”electron”.

[3] H1 uses a right-handed coordinate system with the z-axis along the beam direction, the +z or forward direction being that of the proton beam.

The jet analysis is performed in the Breit frame. The boost from the laboratory system to the Breit frame is determined by Q^2, y and by the azimuthal angle of the scattered electron ϕ_{Lab}. Particles of the hadronic final state are clustered into jets using the inclusive k_T algorithm [2] with the p_T recombination scheme and with the distance parameter $R = 1$ in the $\eta_B - \phi_B$ plane. The cut $-0.8 < \eta_{Lab} < 2.0$ ensures that jets are well contained within the acceptance of the LAr calorimeter, where η_{Lab} is the jet pseudorapidity in the laboratory frame. Every jet with transverse energy in the Breit frame $7 < E_{T,B} < 50$ GeV contributes to the inclusive jet cross section, regardless of the jet multiplicity in the event.

Multi-jet events, also called n-jet events (2-jet or 3-jet are measured) are accepted, if at least n jets with $5 < E_{T,B} < 50$ GeV are reconstructed within the same η_{Lab} range as for the inclusive jets. In addition, a cut on the invariant mass $M_{12} > 16$ GeV of the two leading jets is applied, to define for the NLO calculation an infrared safe cross section.

3 Defintion of normalized cross sections

Jet multiplicities are the normalized inclusive, 2-jet and 3-jet cross sections, calculated as the ratio of the differential inclusive, 2-jet and 3-jet cross sections and the differential NC DIS cross section, multiplied by the $E_{T,B}$ bin width W_{Et} in case of a double differential measurement:

$$\sigma_{jet,N} = \frac{d\sigma^2_{Ijet}/dQ^2 dE_{T,B}}{d\sigma_{NC}/dQ^2} \cdot W_{Et} \qquad (1)$$

$$\sigma_{2-jet,N} = \frac{d\sigma^2_{2-jet}/dQ^2 d < E_{T,B} >}{d\sigma_{NC}/dQ^2} \cdot W_{Et} \qquad (2)$$

4 Monte Carlo models and correction procedure

In order to extract cross sections at hadron level, the experimental data are corrected bin-by-bin for limited detector acceptance and resolution. The correction factors are determined using simulated NC DIS events. The generated events are passed through a detailed simulation of the H1 detector and are subjected to the same reconstruction and analysis chain as the data. The following Monte Carlo event generators are used for this purpose: DJANGOH [5] using the Colour Dipole Model as implemented in ARIADNE [6] and RAPGAP [7] using leading order matrix elements matched to parton showers. Both RAPGAP and DJANGOH provide a good descriptions of the data in both the inclusive DIS and the inclusive jet samples and so describe well jet multiplicities.

The purity of the jet sample, defined as the fraction of jets reconstructed in a bin which are generated in that same bin on hadron level, is found to be larger than 60% in all analysis bins. The same is observed for the stability defined as the fraction of hadron level jets that originate in a bin and are subsequently reconstructed in that bin. A bin-by-bin correction is applied to the raw measured cross sections. Total correction factors, including detector and QED radiation corrections, are determined in one step as the ratio of the cross section obtained from particles at the non-radiative hadron level to the cross section calculated using particles reconstructed from the detector information. Arithmetic means of the correction factors determined by RAPGAP and DJANGOH are used, and half of the difference is assigned as the systematic uncertainty due to the sensitivity of the detailed simulation to the MC model. The correction factors deviate typically by less than 20% from unity. In order to merge positron and electron periods, the data are corrected for Z^0 boson exchange using factors estimated with the LEPTO event generator [8]. Since this correction depends only on Q^2, it cancels to first order in the normalised cross sections. Jet multiplicities are calculated and corrected separately for positron and electron periods and then combined.

5 NLO QCD calculations

The QCD prediction for the jet cross section is calculated using the NLOJET++ program [10], which performs the integration of the matrix elements at NLO in the strong coupling, $O(\alpha_s^2)$. The DIS cross section is calculated at $O(\alpha_s)$ with the DISENT program [11]. The FastNLO package [12] allows a fast convolution of QCD matrix elements with the parton density functions (PDFs) of the proton.

The value for the strong coupling is taken as $\alpha_s(M_Z) = 0.118$ and is evolved as a function of the renormalisation scale at two loop precision. The calculations are performed in the $\overline{MS}$ scheme for five massless quark flavours. The PDFs of the proton are taken from the CTEQ6.5M set [9]. The factorisation scale μ_f is taken to be Q and the renormalisation scale μ_r is taken to be $\sqrt{Q^2 + E_{T,B}^2/2}$ for NLO predictions of cross sections for inclusive jets and Q for cross sections of 2-jet, 3-jet and DIS. The running of the electromagnetic coupling with Q^2 is also taken into account. No QED radiation is included in the calculation, since the data are corrected for this effect.

Jet cross-sections are predicted at the parton level using the same jet definition as in the data analysis. For comparison with the data, hadronisation corrections are calculated for each bin as the ratio of the cross section defined at hadron level to the cross section defined at parton level. These correction factors are determined with the same Monte Carlo event samples from DJANGOH and RAPGAP used to correct the data from detector to hadron level (see 4). The hadronisation correction factors differ typically by less than 10% from unity and agree at the level of 2% between the two Monte Carlo simulations.

The theoretical uncertainties (or error band) shown in the figures include an uncertainty for hadronisation and an estimate of the uncertainty due to missing higher orders in the perturbative calculation. The systematic error attributed to the hadronisation correction is taken to be half of the difference between the correction factors obtained using RAPGAP and DJANGOH. The dominant uncertainty is due to the NLO uncertainty and is conventionally estimated by a separate variation of the chosen scales for μ_f and μ_r by factors within the range of 0.5 to 2. In seven out of the 24 bins in Q^2 and E_T the dependence of the pQCD calculation on μ_r is not monotone, i.e. the largest deviation from the central value is found for factors within the range 0.5 to 2. In such cases the difference between maximum and minimum cross sections found in the variation interval is taken, in order not to underestimate the scale dependence. Renormalisation and factorisation scale uncertainities are added in quadrature. The uncertainty originating from the PDFs is also taken into account using the CTEQ6.5M set of parton densities. The propagation of scale and PDF uncertainties to the cross sections is efficiently performed with the FastNLO program.

The scale uncertainties for the jet and for the NC DIS cross-sections are assumed to be uncorrelated. Consequently, the scale uncertainty for the ratio is estimated by adding the two contributions in quadrature.

6 Results

The normalised inclusive jet cross section or jet multiplicity as a function of Q^2 is shown in figure 1 and the double differential result as a function of E_T in 6 ranges of Q^2 in figure 2. They are compared with NLO calculations and a published measurement by H1 based on HERA I data.

Normalised 2-jet and 3-jet cross sections as a function of Q^2 and their comparison to NLO are shown in figure 3. Figure 4 shows the double differential 2-jet cross sections compared to the NLO calculation.

Values of α_s extracted by fitting the indivdual normalised inclusive jet, 2-jet and 3-jet cross sections and from their combination are shown in figures 5 to 10.

Values for $\alpha_s(M_Z)$ are extracted by fitting the normalised inclusive, 2-jet and 3-jet cross sections individually and by fitting all of them simulateously. The values obtained are given in the table below.

Measurement	$\alpha_S(M_Z)$	exp.error	scale error		PDF error	χ^2/ndf
$\sigma_{Incl.JET}/\sigma_{DIS} = f(Q^2, E_T)$	0.1196	0.0010	+0.0049	-0.0036	0.0019	26.8/23
$\sigma_{2JET}/\sigma_{DIS} = f(Q^2, < E_T >)$	0.1171	0.0010	+0.0048	-0.0036	0.0018	28.1/23
$\sigma_{3JET}/\sigma_{DIS} = f(Q^2)$	0.1179	0.0014	+0.0056	-0.0034	0.0009	4.53/5
$\sigma_{Incl.JET}/\sigma_{DIS}, \sigma_{2JET}/\sigma_{DIS}$, $\sigma_{3JET}/\sigma_{DIS}$	0.1182	0.0008	+0.0041	-0.0031	0.0018	55.8/53

Table 1: Values of $\alpha_S(M_Z)$ obtained from a fit of to the individual normalised inclusive jet, 2-jet and 3-jet cross sections and from a simultaneous fit to all of them.

References

[1] Bassler U and Bernardi G 1995 *NIM* A **361** 197 (*Preprint* hep-ex/9412004).

[2] S. D. Ellis and D. E. Soper, Successive combination jet algorithm for hadron collisions, 301 Phys. Rev. D 48 (1993) 3160 [hep-ph/9305266]; S. Catani et al., Longitudinally Invariant 302 K(T) Clustering Algorithms For Hadron Hadron Collisions, Nucl. Phys. B 406 (1993)

[3] Aktas A *et al.* 2007 *DESY 07-073* (*Preprint* arXiv:0706.3722v2)

[4] Chekanov S *et al.* 2007, *Nucl. Phys.* B **765** 1–30 (*Preprint* hep-ex/0608048)

[5] K. Charchula, G. A. Schuler and H. Spiesberger, Combined QED and QCD radiative effects in deep inelastic lepton - proton scattering: The Monte Carlo generator DJANGO6, Comput. Phys. Commun. 81 (1994) 381.

[6] L. Lonnblad, Ariadne Version 4: A Program For Simulation Of QCD Cascades Implementin The Color Dipole Model, Comput. Phys. Commun. 71 (1992) 15.

[7] H. Jung, Hard diffractive scattering in high-energy e p collisions and the Monte Carlo generation RAPGAP, Comput. Phys. Commun. 86 (1995) 147.

[8] G. Ingelman, A. Edin and J. Rathsman, LEPTO 6.5, Comput. Phys. Commun. 101 (1997) 108 [hep-ph/9605286].

[9] J. Pumplin et al., New generation of parton distributions with uncertainties from global QCD analysis, JHEP 0207 (2002) 012 [hep-ph/0201195];

W. K. Tung et al., Heavy quark mass effects in deep inelastic scattering and global QCD analysis, [hep-ph/0611254].

[10] Nagy Z and Trocsanyi Z 2001, *Phys. Rev. Lett.* 87 082001 (*Preprint* hep-ph/0104315)

[11] S. Catani and M. H. Seymour, Nucl. Phys. B 485 (1997) 291 [Erratum-ibid. B 510 (1998) 503] [hep-ph/9605323].

[12] Kluge T, Rabbertz K and Wobisch M *Preprint* hep-ph/0609285

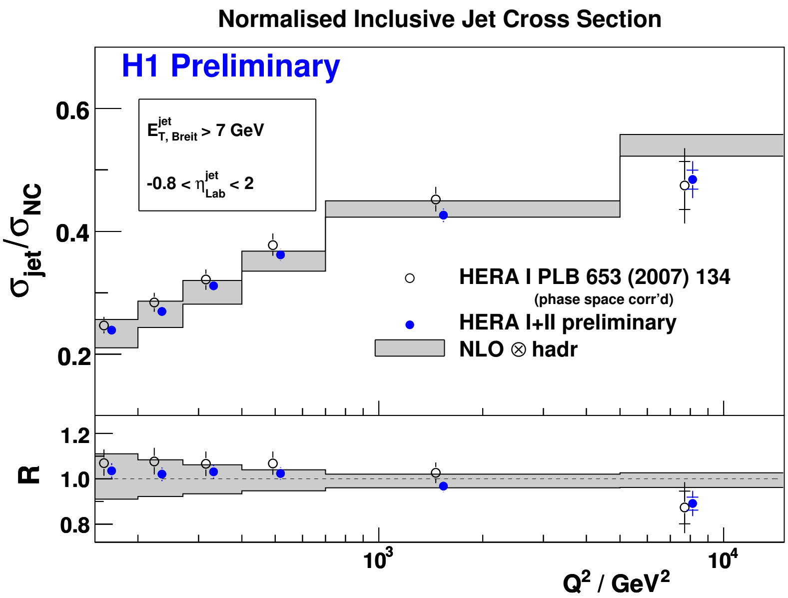

Figure 1: Jet multiplicities as a function of Q^2 measured with HERA I and HERA II combined data samples compared to HERA I published data, here shown corrected for phase space. The NLO QCD predictions together with the theory uncertainty associated with the renormalisation and factorisation scales, PDF uncertainty and the hadronisation corrections are shown as the grey band. The ratio R of data with respect to the NLO QCD prediction is shown on the lower plot.

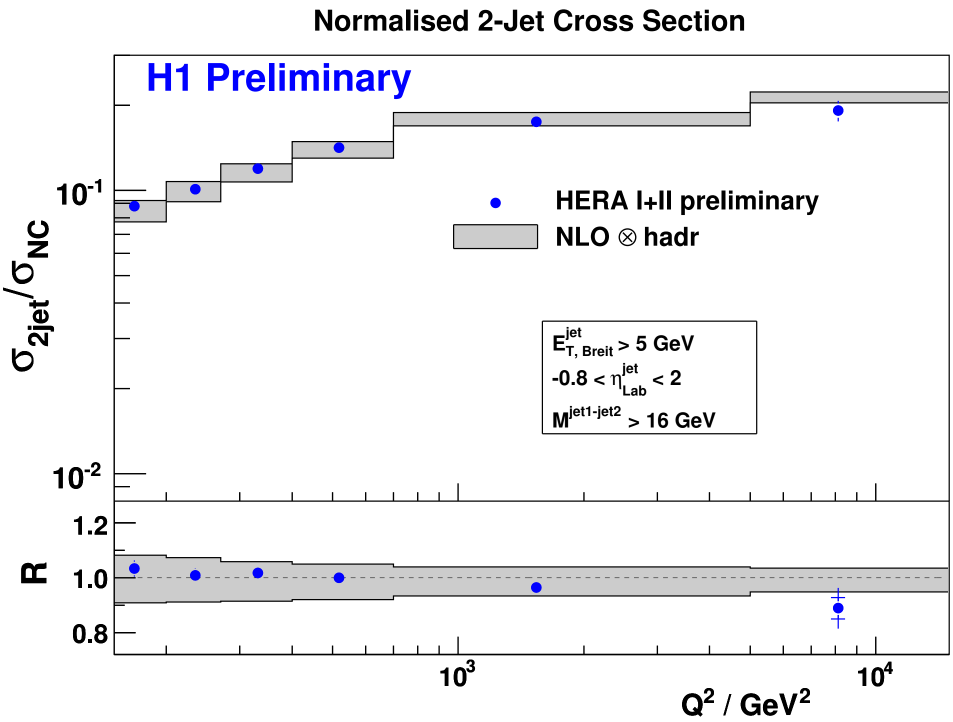

Figure 2: Jet multiplicities as a function of $E_{T,B}$ in regions of Q^2 measured with HERA I and HERA II combined data samples compared to HERA I published data, here shown corrected for phase space. The NLO QCD predictions together with the theory uncertainty are shown as the grey band. The ratio R of data with respect to the NLO QCD prediction is shown on the lower plots.

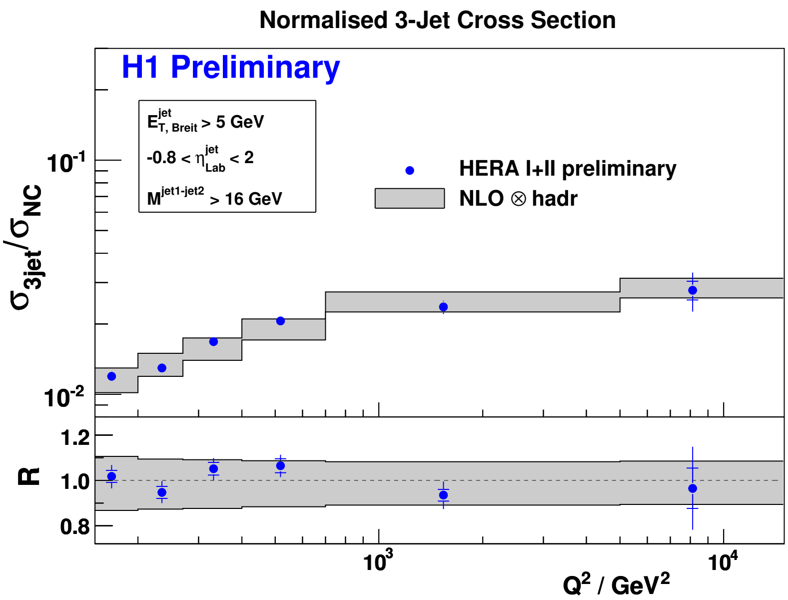

Figure 3: 2-jet rates as a function of Q^2 measured with HERA I and HERA II combined data samples. The NLO QCD predictions together with the theory uncertainty associated with the renormalisation and factorisation scales, PDF uncertainty and the hadronisation corrections are shown as the grey band. The ratio R of data with respect to the NLO QCD prediction is shown on the lower plots.

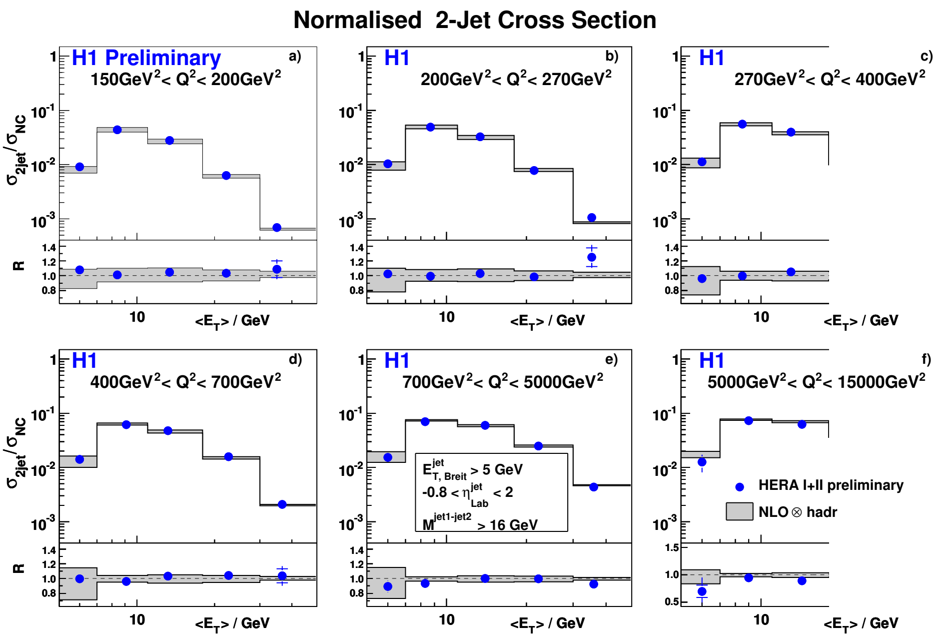

Figure 4: 3-jet rates as a function of Q^2 measured with HERA I and HERA II combined data samples. The NLO QCD predictions together with the theory uncertainty associated with the renormalisation and factorisation scales, PDF uncertainty and the hadronisation corrections are shown as the grey band. The ratio R of data with respect to the NLO QCD prediction is shown on the lower plots.

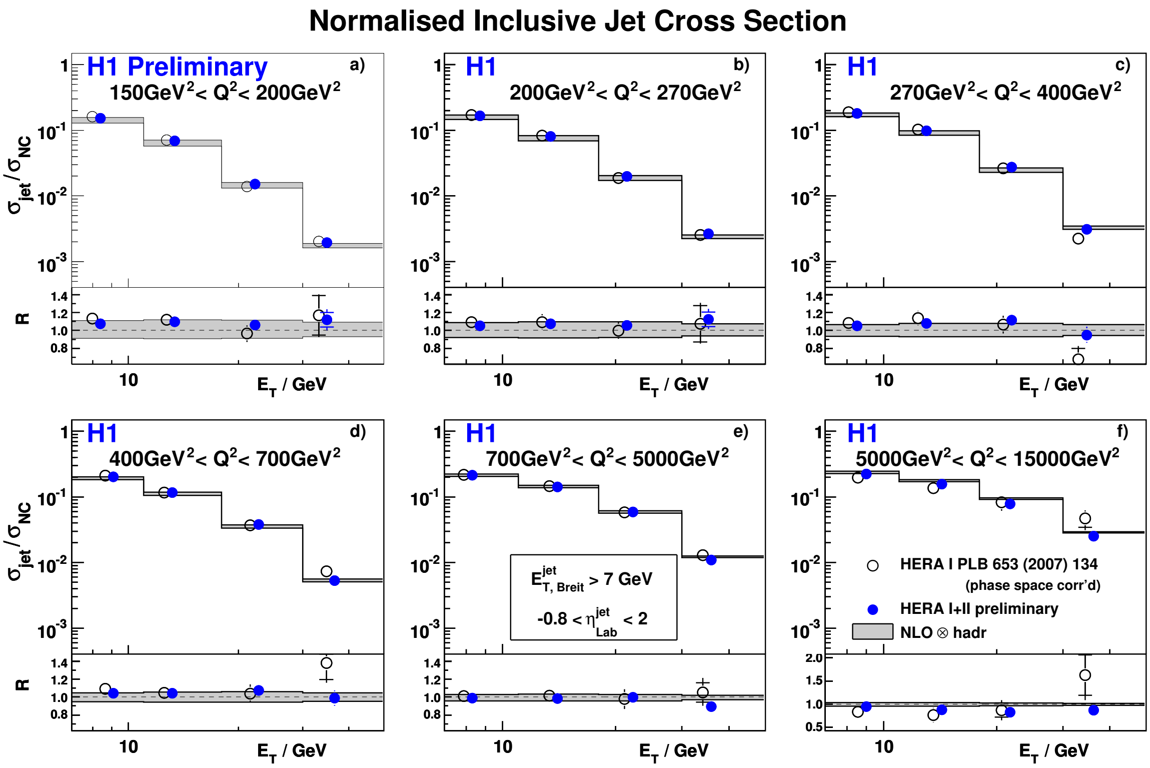

Figure 5: 2-jet rates as a function of $E_{T,B}$ in regions of Q^2 measured with HERA I and HERA II combined data samples. The NLO QCD predictions together with the theory uncertainty associated with the renormalisation and factorisation scales, PDF uncertainty and the hadronisation corrections are shown as the grey band. The ratio R of data with respect to the NLO QCD prediction is shown on the lower plots.

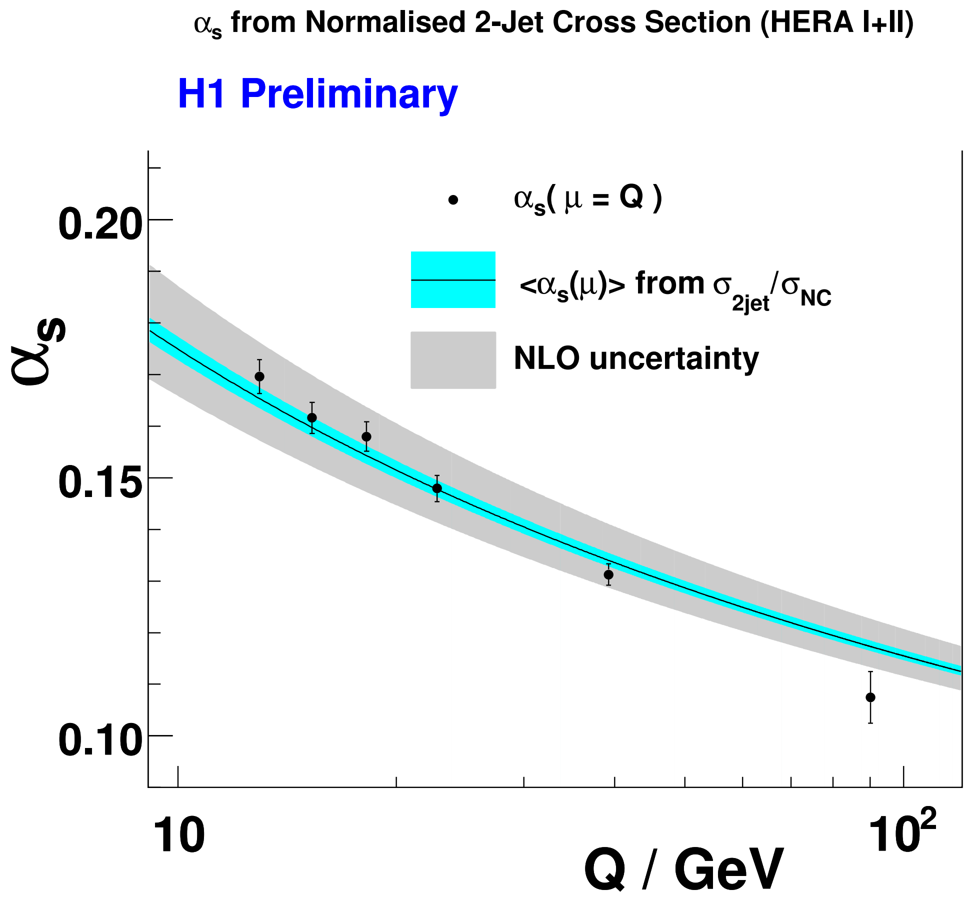

Figure 6: Results of the fitted values of $\alpha_s(E_T)$ using the inlcusive jet multiplicities for six regions of Q^2. The error bar denotes the total experimental uncertainty of each data point. The solid line shows the two loop solution of the renormalisation group equation, evolving the $\alpha_s(M_Z)$ obtained from a fit of 24 measurements of the inclusive jet multiplicities as function of Q^2 and $< E_T >$, with the inner the grey band denoting the theoretical uncertainties associated with the renormalisation and factorisation scales, PDF uncertainty and the hadronisation corrections.

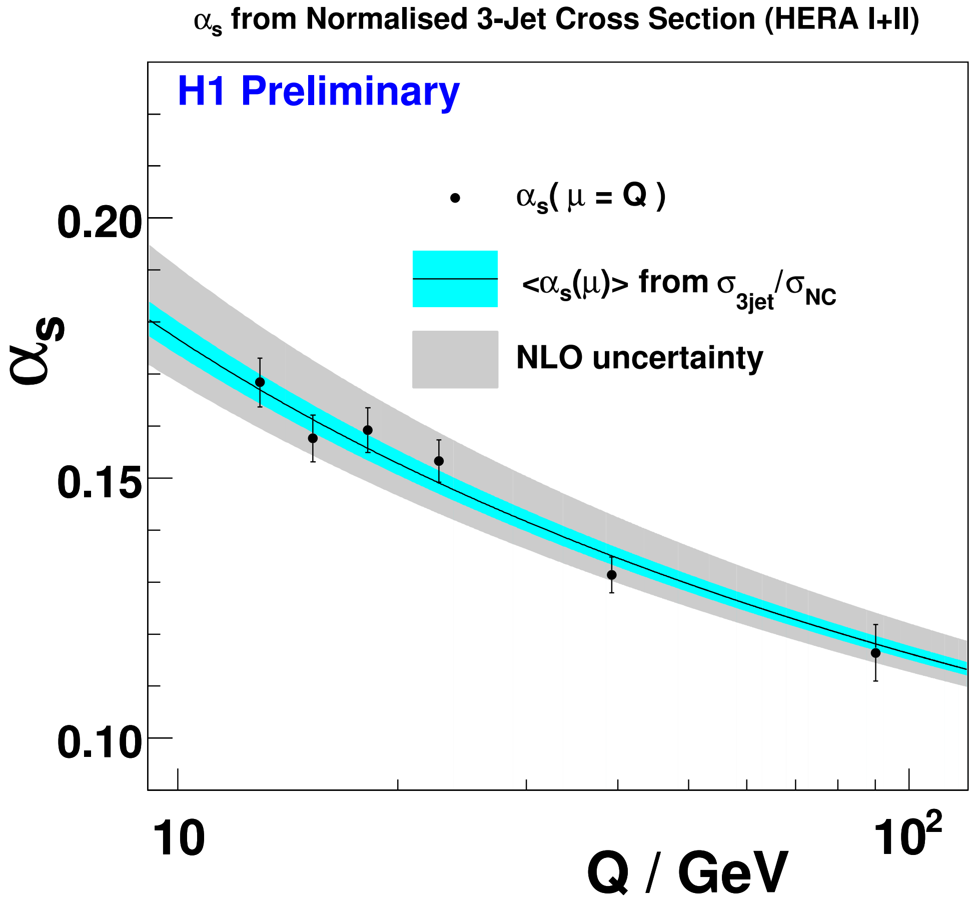

Figure 7: Results of the fitted values of $\alpha_s(\mu = Q)$ averaged over all E_T regions. The error bar denotes the total experimental uncertainty of each data point. The solid line shows the two loop solution of the renormalisation group equation evolving the $\alpha_s(M_Z)$ obtained from a fit of 24 measurements of the inclusive jet multiplicities measured as function of Q^2 and E_T, with the inner blue band denoting the correlated experimental uncertainties and the grey band denoting the theoretical uncertainties associated with the renormalisation and factorisation scales, PDF uncertainty and the hadronisation corrections.

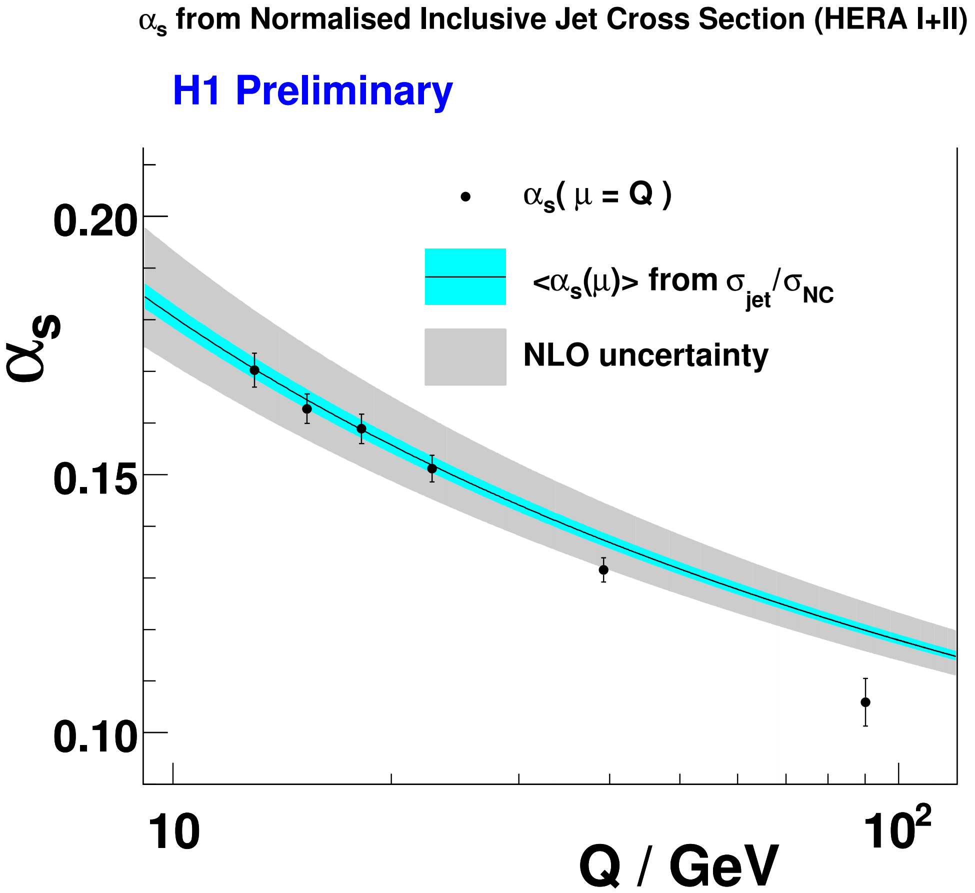

Figure 8: Results of the fitted values of $\alpha_s(\mu = Q)$ averaged over all $< E_T >$ regions. The error bar denotes the total experimental uncertainty of each data point. The solid line shows the two loop solution of the renormalisation group equation evolving the $\alpha_s(M_Z)$ obtained from a fit of 24 measurements of the 2-jet rates measured as function of Q^2 and $< E_T >$, with the inner blue band denoting the correlated experimental uncertainties and the grey band denoting the theoretical uncertainties associated with the renormalisation and factorisation scales, PDF uncertainty and the hadronisation corrections.

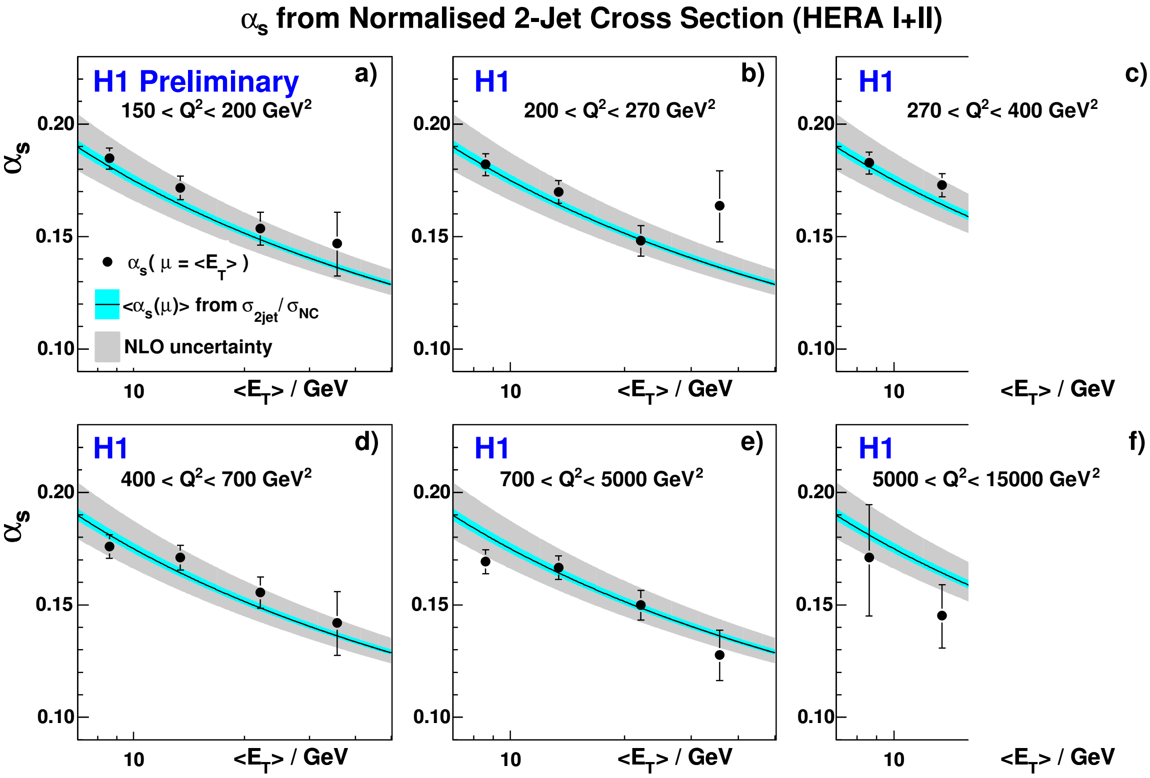

Figure 9: Results of the fitted values of $\alpha_s(E_T)$ using the 2-jet rates for six regions of Q^2. The error bar denotes the total experimental uncertainty of each data point. The solid line shows the two loop solution of the renormalisation group equation evolving the $\alpha_s(M_Z)$ obtained from a fit of 24 measurements of 2-jet rates as function of Q^2 and $< E_T >$, with the inner blue band denoting the correlated experimental uncertainties and the grey band denoting the theoretical uncertainties associated with the renormalisation and factorisation scales, PDF uncertainty and the hadronisation corrections.

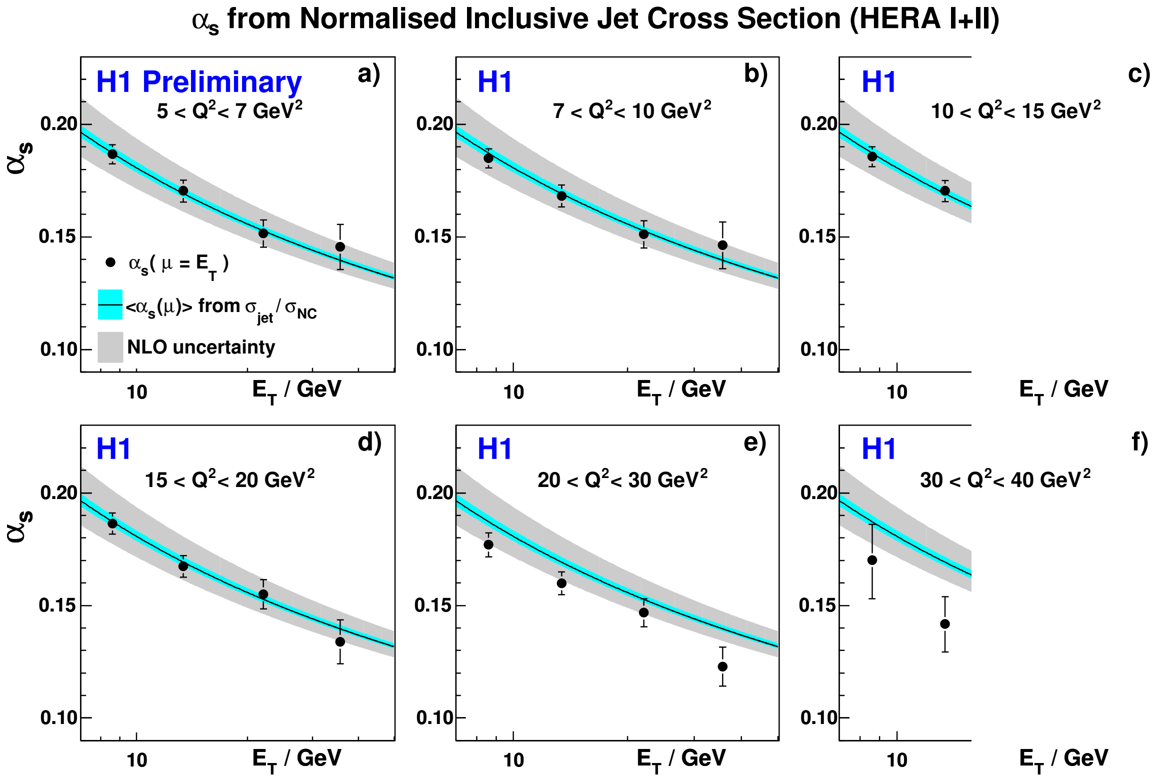

Figure 10: Results of the fitted values of $\alpha_s(\mu = Q)$. The error bar denotes the total experimental uncertainty of each data point. The solid line shows the two loop solution of the renormalisation group equation evolving the $\alpha_s(M_Z)$ obtained from a fit of 6 measurements of the 3-jet rates measured as function of Q^2, with the inner blue band denoting the correlated experimental uncertainties, and the grey band denoting the theoretical uncertainties associated with the renormalisation and factorisation scales, PDF uncertainty and the hadronisation corrections.

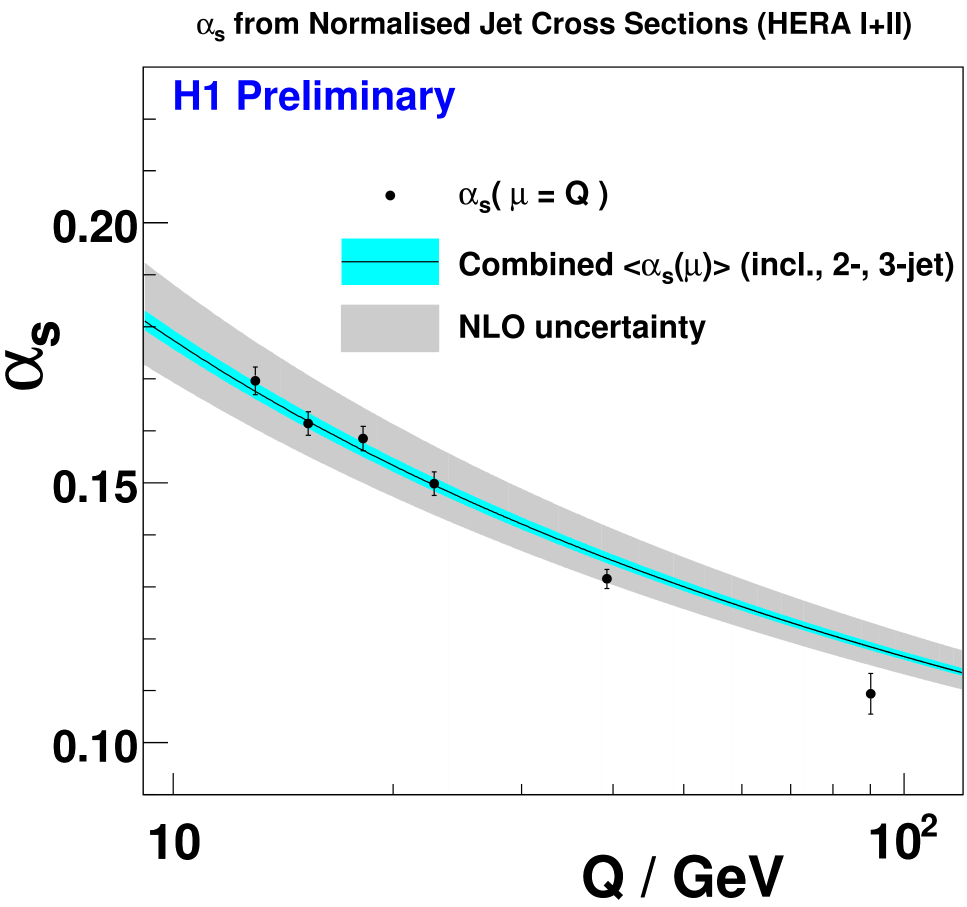

Figure 11: Results of the fitted values of $\alpha_s(\mu = Q)$. The error bar denotes the total experimental uncertainty of each data point. The solid line shows the two loop solution of the renormalisation group equation evolving the $\alpha_s(M_Z)$ obtained from a fit of 54 measurements of the inclusive jet multiplicities as function of Q^2 and E_T, 2-jet rates as function of Q^2 et $< E_T >$ and finally 3-jet rates as function of Q^2, with the inner blue band denoting the correlated experimental uncertainties, and the grey band denoting the theoretical uncertainties associated with the renormalisation and factorisation scales, PDF uncertainty and the hadronisation corrections.